

EIGEN DECOMPOSITION PARAMETER BASED FOREST MAPPING USING RADARSAT-2 POLSAR DATA

Yang Li^{1,2}, Wen Hong^{1,2}, Fang Cao^{1,2}, Erxue Chen³, David G. Goodenough^{4,5}, Hao Chen⁴, Peng Wang^{1,2}, Ashlin Richardson⁴

¹National Key Laboratory of Microwave Imaging Technology, Beijing, 100190, P.R. China

²Institute of Electronics, Chinese Academy of Sciences

³Institute of Forest Resources Information Techniques, Chinese Academy of Forestry

⁴Pacific Forestry Centre, Natural Resources Canada

⁵Department of Computer Science, University of Victoria, Victoria, BC, Canada

No.19 Bei Si Huan Xi Lu, Beijing, China, 100080

(Tel: 86-10-5888-7104 Fax : 86-10-5888-7526 Email: liyang@mail.ie.ac.cn)

ABSTRACT

In this paper, a set of polarimetric eigenvalue and eigenvector based parameters, e.g. entropy and anisotropy, are investigated for forest application. However, only μ_1 and μ_2 are found to be effective for forest mapping in both summer and winter using Radarsat-2 quad-polarimetric space borne SAR dataset. This characteristic is used to automatically pick up forest class pixels from the volume scattering category of Freeman-Durden Wishart unsupervised segmentation map. The algorithm scheme is developed and implemented using the fully polarimetric SAR (PolSAR) data acquired in July and October and the validity is evaluated using the ground reference data created from SPOT5 K-clustering classification map.

Index Terms— Forest mapping, Radarsat-2, Polarimetric, eigenvalue, classification

1. INTRODUCTION

Radarsat-2 is the first active C-band space-borne SAR sensor with fully polarimetric (PolSAR) data receiving capability. There are roles for Radarsat-2 in forestry applications. By providing alternate information and augmenting other data sources for forest uses, Radarsat-2 will contribute to national programs on global warming and carbon emissions. Key components of these are monitoring forest change, estimating biomass, and providing forest type classifications. Due to the short wavelength of the C-band PolSAR data, the SAR backscatter sigma value or intensity saturates quickly compared to PolSAR data at L- or P-band. However, the above applications may be achieved through the benefit of polarimetric eigenvector analysis. In this paper, we will introduce roll-invariant parameters derived from the correlation of the eigenvector terms. The use of these parameters makes it possible to map forest areas and

monitor forest change from space with C-band polarimetric SAR. The polarimetric decomposition theorem provides a reasonable scheme to characterize the scattering behavior of pure target and the dominant contribution of random media [1]. Based on this scheme, we found the second term real part of dominant eigenvector presents a great potential for distinguishing forest and non-forest areas at C-band, which is very useful to separate forest from clear-cut, fire scars and vegetation areas without threshold value estimation. This property reveals strong adaptability to a wide range of time variation.

2. STUDY SITES AND DATA SETS

Ta-He forestry study site in Heilongjiang province, the northeast border of China, is selected for the forest mapping experiment. The study site in Figure 1 shows general topographic features and great difference between the two data acquiring seasons, July and October. There was a wild forest fire that occurred on September 29th, 2001 over this area, much broader than Figure 1 covers.

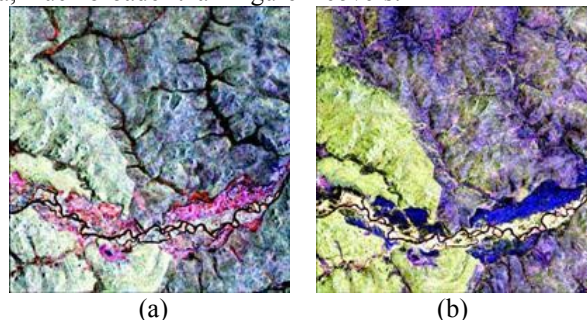


Figure 1 (a) PolSAR image (dB) of Ta-He in July (b) PolSAR image (dB) of Ta-He in October. (Red= $|HH-HV|$, Green= $|HV|$, Blue= $|HH+VV|$)

A SPOT5 Level 1A image is used as ground truth reference. This data set was collected on July 27th, 2006, and has a

panchromatic channel with a 2.5m resolution and multi-spectral channels with a 10m spatial resolution. The orthorectified K-clustering classification map is displayed in Figure 2 (a). For comparison, we choose the forest classes manually from Figure 2 (a) and match it with the two radar images by projecting it into radar domain as a forest cover reference map displayed in Figure 2 (b).

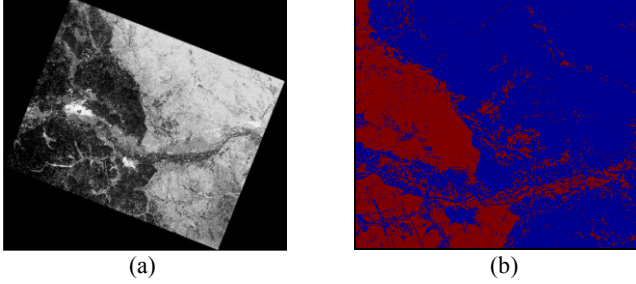


Figure 2 (a) Classification image using SPOT5 data (b) Forest cover reference map in radar domain, Red=forested area.

3. EIGEN DECOMPOSITION PARAMETER

The 3×3 polarimetric coherency matrix T can be presented by the product of eigenvalues and eigenvectors, i.e.

$$T = \sum_{i=1}^3 \lambda_i u_i \cdot u_i^{*T} \quad (1)$$

where λ_i are the eigenvalues of T , $\lambda_1 \geq \lambda_2 \geq \lambda_3 \geq 0$ represent the statistical weight and the order of three kinds of scattering mechanisms. The unit orthogonal eigenvectors u_i can be written as

$$u_i = [u_{1i}, u_{2i}, u_{3i}]^T = e^{j\phi_i} [\cos \alpha_i, \sin \alpha_i \cos \beta_i e^{j\delta_i}, \sin \alpha_i \sin \beta_i e^{j\gamma_i}]^T \quad (2)$$

The radar vegetation index (RVI) has been introduced by Van Zyl [2] and is used to differentiate forest area from other scattering media. This parameter describes the size of cylinders, ranging from 0 to $4/3$.

$$RVI = 4\lambda_3 / (\lambda_1 + \lambda_2 + \lambda_3) \quad (3)$$

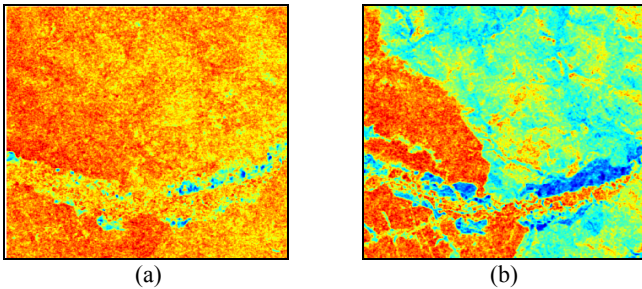


Figure 3 (a) The radar vegetation index in July (b) The radar vegetation index in October.

In addition to the RVI and four angles in (2), we also have tried other eigenvalue and eigenvector based polarimetric scattering parameters including the polarimetric entropy, the alpha angle, the anisotropy, the SERD, the DERD and so on which are summarized well in [3]. Most of them have the similar performance with RVI in Figure 3 on differentiating

the forested area from the other media especially over the fired area. It's easy to separate the two kinds of areas in the winter image (Figure 3(b)) if we set a credible threshold because their polarimetric scattering categories are totally different, one is volume scattering and the other one is surface scattering. However, considering to the C-band PolSAR data penetrating ability, the covered vegetation e.g. grass, growing well in July makes the difference little because the forested and fired area character all belong to the volume scattering. Therefore, it's difficult to get the forest map by setting threshold value merely.

The other parameter, used to map forest displayed in Figure 4, is the correlation term real part of the first eigenvector, i.e.

$$\mu_1 = \text{real}(\langle u_{21} \cdot u_{11}^* \rangle / \langle |u_{21}| \cdot |u_{11}| \rangle) \quad (4)$$

The forested areas are found corresponding to the pixels that satisfy $\mu_1 < 0$. The correlation term real part of the second eigenvector μ_2 and the anisotropy A is used to exclude the pixels which belong to water bodies.

$$\mu_2 = \text{real}(\langle u_{22} \cdot u_{12}^* \rangle / \langle |u_{22}| \cdot |u_{12}| \rangle) \quad (5)$$

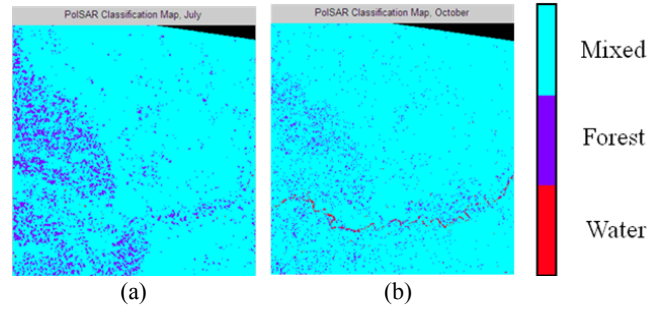


Figure 4 (a) Ta-He classification map based on μ in July (b) Ta-He classification map based on μ in October.

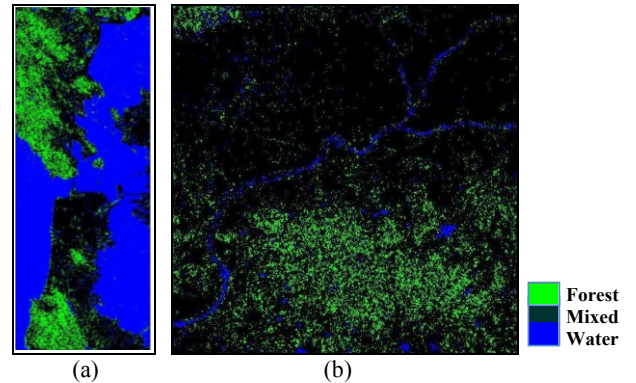


Figure 5 (a) Golden Gate, San Francisco classification map based on μ (b) Culai Mountain classification map based on μ in August.

The preliminary classification maps in Figure 4 indicate that parameter μ can be used to forest mapping no matter in summer or winter but not good enough. We also test this parameter using Radarsat-2 data over San Francisco, U.S.A. (Figure 5 (a)) and Culai Mountain in Shandong, China (Figure 5 (b)); hence we propose a method makes use of

parameter μ to automatically get forest class pixels from the Freeman-Durden Wishart classification map.

4. FOREST MAPPING WITH FREEMAN-DURDEN WISHART CLASSIFICATION RESULTS

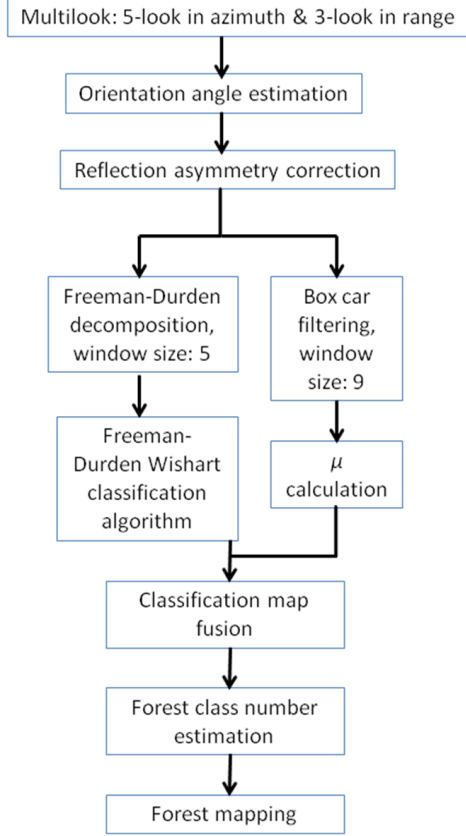


Figure 6 Forest mapping workflow scheme using Radarsat-2 PolSAR data

The flowchart of our forest mapping method is illustrated in Figure 6 which is composed by the reflection asymmetry correction [4], the Freeman-Durden Wishart classification algorithm [5, 6], and the forest class label estimation.

The reflection symmetry condition as a basic assumption of the Freeman-Durden's three-component decomposition must be satisfied. Commonly, the reflection asymmetry effect of longer wave SAR data is induced by non-flat surface structures, such as topography, branches and leaves. For Radarsat-2 C-band SAR, the shorter wavelength return is more sensitive to the vegetation canopy than rough surfaces beneath the canopy. To perform compensation, a polarization orientation angle (POA) shift is estimated according to Equation (6) and (7) [7]:

$$\eta = \frac{1}{4} \left[\tan^{-1} \left(\frac{-4 \operatorname{Re}(\langle \tilde{S}_{HH} - \tilde{S}_{VV} \rangle \tilde{S}_{HV}^*)}{- \langle |\tilde{S}_{HH} - \tilde{S}_{VV}|^2 \rangle + 4 \langle |\tilde{S}_{HV}|^2 \rangle} \right) + \pi \right] \quad (6)$$

$$\theta = \begin{cases} \eta, & \text{if } \eta \leq \pi/4 \\ \eta - \pi/2, & \text{if } \eta > \pi/4 \end{cases} \quad (7)$$

where θ is the POA shift, and \tilde{S}_{xy} is the polarimetric SAR scattering matrix term. Next, the reflection asymmetry effect is compensated by removing the effect of the POA shift from the coherency matrix T using Equation (8) [7].

$$T^{new} = UTU^T, U = \begin{bmatrix} 1 & 0 & 0 \\ 0 & \cos 2\theta & \sin 2\theta \\ 0 & -\sin 2\theta & \cos 2\theta \end{bmatrix} \quad (8)$$

An advantage of this compensation algorithm is that it depends only upon the coherency matrix T but not any other data sources.

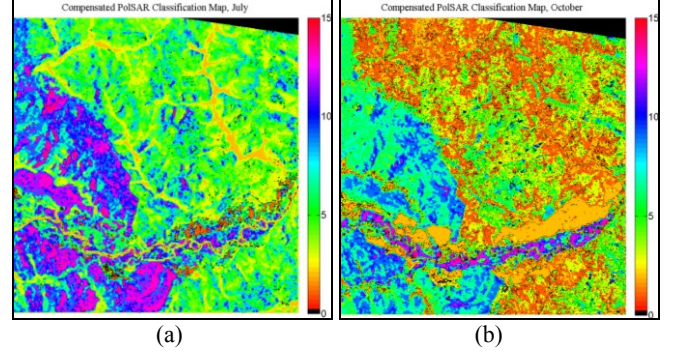


Figure 7 (a) Freeman-Durden Wishart segmentation map in July (b) Freeman-Durden Wishart segmentation map in October.

The polarization information contained in fully polarimetric SAR data sets shows great potential for measuring forest scattering characteristics and producing separation between different forest areas for forest type discrimination, clear-cut and fire scar delineation. Forests have strong volume scattering; burned areas show relatively strong surface scattering with mixed volume and double bounce scattering; clear cuts and farmer's lands all have strong surface scattering. Our study is focused on exploring effective classification methods (based on the scattering characteristics) for the identification of forest area in the study region no matter in summer or winter. The Wishart classification scheme with different approaches has been investigated and studied, especially with the Freeman-Durden three-component decomposition initialization [5, 6]. The initialization for the Wishart classification using the Freeman-Durden decomposition separates the polarimetric SAR data into three categories of pixels that are each dominated by the following scattering mechanisms: single bounce, double bounce, and volume scattering, respectively. Throughout the algorithm, the data remains separated in this way. Next, the pixels are divided according to their power into a large number of small seed classes, each containing an equal number of pixels; the small seed classes are merged together (within each of the scattering categories) based on the between-class Wishart distance [6]. Since the pixels in the three categories are kept separate from one another, this unsupervised terrain classification produces the classes that contain pixels with the same type of a scattering mechanism.

The Ta-He segmentation maps are shown in Figure (7). The terrain relief variation effect is still clear in both two maps. It's easy to get the forest map from them manually but impossible to the summer map. However, we can combine them with the classification maps in Figure 4 as shown in Figure 8. The class label histogram plots after filtering are shown in Figure 9.

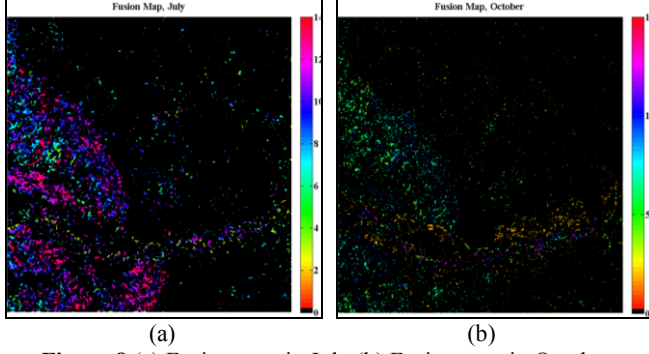


Figure 8 (a) Fusion map in July (b) Fusion map in October.

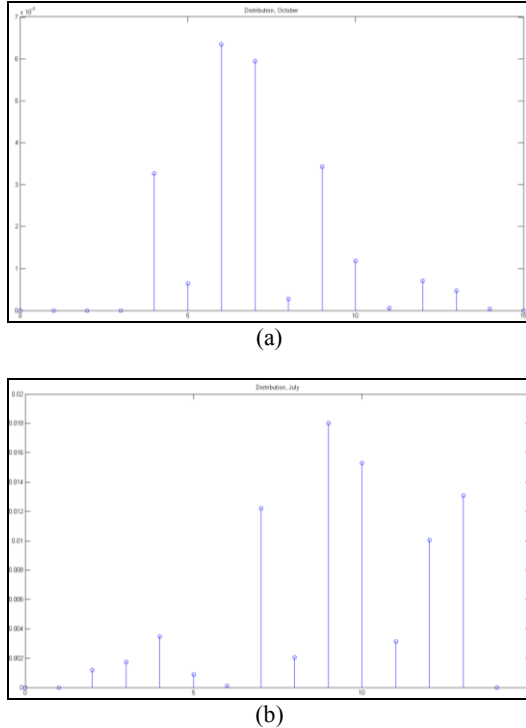


Figure 9 (a) Filtered class label distribution plot in July, processed (b) Filtered class label distribution plot in October.

Next step, we can find out the label corresponding to the max value in Figure 9 as label 1, which means the label with most pixels in Figure 8 and we also know the last label of volume scattering category from Figure 7 as label 2. Finally, we pick up all the pixels labeled between label 1 and label 2 from Figure 7 and that is the forest map, as shown in Figure 10. Compared with Figure 2 (b), the accuracy is 66.98% in summer and 80.32% in winter.

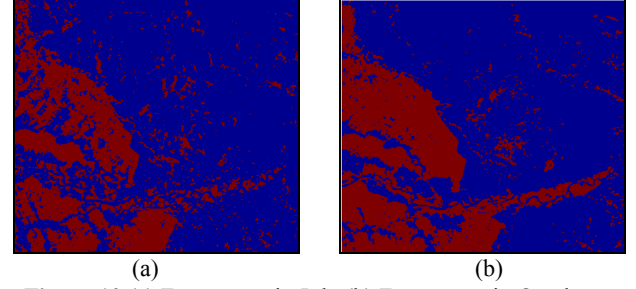


Figure 10 (a) Forest map in July (b) Forest map in October. Red=forested area.

5. CONCLUSION

The eigenvalue parameter μ and the Freeman-Durden Wishart classification algorithm are used to map forested areas automatically. The preliminary study results over Ta-He study site indicate that the C-band Radarsat-2 fully polarimetric SAR potential for global forest mapping no matter in summer or winter. The validity of the results is evaluated using the ground reference data created from SPOT5. The terrain effect should be further removed.

6. ACKNOWLEDGEMENT

This work was supported by the National Natural Science Foundation of China Key Program (Grant. NO. 60890071) and BC-China ICSD Program (2008DFA11690).

7. REFERENCES

- [1] S. R. Cloude, and E. Pottier, "An entropy based classification scheme for land applications of polarimetric SAR", Transactions on Geoscience and Remote Sensing, vol. 35, no. 1, pp. 68-78, Jan. 1997.
- [2] Van Zyl J.J., H.A. Zebker, and C. Elachi, "Imaging radar polarization signatures", Radio Science, 22, 529-543, 1987.
- [3] Jong Sen Lee., Eric Pottier, "Polarimetric Radar From Basics to Applications", CRC Press, 2009.
- [4] David G. Goodenough, Wen Hong et. al, "Mapping Fire Scars From Space Using Radarsat-2 Polarimetric SAR", ASTRO 2010, Toronto, Canada, May 4-6, 2010.
- [5] A. Freeman and S. L. Durden, "A three-component scattering model for polarimetric SAR data", IEEE Transactions on Geoscience and Remote Sensing, vol. 36, no. 3, pp. 936-973, May 1998.
- [6] J. S. Lee, M. R. Grunes, E. Pottier, and L. Ferro-Famil, "Unsupervised terrain classification preserving polarimetric scattering characteristics", IEEE Transactions on Geoscience and Remote Sensing, vol.42, issue 4, pp.722-731, 2004.
- [7] J. S. Lee, D. L. Schuler, and T. L. Ainsworth, "Polarimetric SAR Data Compensation for Terrain Azimuth Slope Variation", IEEE Transactions on Geoscience and Remote Sensing, vol. 38, no. 5, pp. 2153-2163, Sep. 2000.